ELSEVIER

International Journal of Mass Spectrometry 192 (1999) 9–22

International Journal of Mass Spectrometry

Plasma rate coefficients for highly charged ion–electron collisions: new experimental access via ion storage rings

Alfred Müller*

Institut für Kernphysik, Strahlenzentrum der Justus-Liebig-Universität, D-35392 Giessen, Federal Republic of Germany

Received 26 November 1998; accepted 13 April 1999

Abstract

Collisions of electrons with ions govern the dynamics and the radiative properties of plasmas whether they are of natural or laboratory origin. Knowledge about collision rate coefficients is essential for the modeling and understanding of any kind of plasma. During recent years heavy ion storage rings have proven to be outstanding tools for detailed measurements of cross sections and rates for electron impact ionization and recombination of ions in any given charge state ranging from H^- up to U^{92+}. Thus, storage ring experiments with colliding electron and ion beams provide unique new access to atomic data, which are needed for plasma applications. As an example, rate coefficients for ionization and recombination of Fe^{15+} ions are determined and compared with previously recommended data. (Int J Mass Spectrom 192 (1999) 9–22) © 1999 Elsevier Science B.V.

Keywords: Highly charged ions; Electron collisions; Plasma rate coefficients; Storage rings

1. Introduction

Charge-changing electron–ion collisions, i.e. ionization and recombination, involve fundamental atomic interactions. Studying details of these processes enhances our understanding of the quantum-physical basis of nature and provides knowledge about the structure and the dynamics of atomic particles. Besides their intrinsic relevance, however, electron–ion collisions are also most important in plasma applications. They determine the charge-state balance of atoms in ionized gas and, hence, also the spectrum of electromagnetic radiation emitted by that gas. Understanding and diagnosing the state of a plasma, whether of astrophysical origin or man made, relies on information about cross sections and rate coefficients for electron–ion interactions.

Colliding beams of electrons and ions [1] have been used for almost 40 years for studies of electron–ion collision processes. By far the most of the available data—preferably on ionization—were obtained with small-scale equipment, i.e. with an ion source on an electrostatic potential of typically several kilovolts, providing beams of slow ions, and with an (intersecting) electron beam of electron volt to kiloelectron volt energies in combination with the necessary equipment to characterize the beams and their overlap and to accomplish signal recovery. To date, information on electron-impact excitation of ions is almost exclusively based on such experiments.

By the combination of the well known merged beams approach with ion accelerator technology a

* Corresponding author. E-mail: Alfred.Mueller@strz.uni-giessen.de

1387-3806/99/$20.00 © 1999 Elsevier Science B.V. All rights reserved
PII S1387-3806(99)00098-6

new era of electron–ion collision studies began little over a decade ago [2]. Nine heavy ion storage rings equipped with electron cooling devices have become available world wide [3]. The majority of these devices are concentrated in Europe. They provide new unique possibilities to study electron–ion collisions with high precision in a wide parameter range. By merging bright, cooled ion beams with very cold intense and well characterized electron beams of the cooling device, energies in the electron–ion center-of-mass frame from 0 to several kiloelectron volts are presently accessible. Energy spreads as low as approximately 10 meV have been experimentally verified at low energies. Intense ion beams (up to 1 mA of completely stripped uranium) can presently be made available, depending on the choice of accelerator facility. Four of the rings (TSR in Heidelberg, ESR in Darmstadt, ASTRID in Aarhus, and CRYRING in Stockholm) have devoted most of their beam time to atomic physics. They provide complementing opportunities for experiments. The author and his collaborators have taken advantage of these opportunities at several different storage rings to study charge-changing electron–ion collisions covering ionization and recombination of many ions in the whole range between Li^+ and U^{89+} [4].

In spite of the numerous experimental facilities—small scale or accelerator based—that have been set up by now for electron–ion collision studies and in spite of the steadily improving technology, experiment will never be able to provide all the data that are needed in modeling a plasma like the solar corona. Only theory and empirical scaling can provide the huge amount of atomic collision and structure data entering a realistic plasma modeling code. In fact, experiments studying electron–ion collisions in the laboratory have even not become possible until the early 1960's while theory on electron collision phenomena (which—for neutral atoms—is not all that much different from the theory for ions) had already been developed for decades. Because of the limitations on the experimental side and the pressing data needs of astrophysics and plasma fusion research it was necessary to construct data bases for plasma rate coefficients by using predominantly theoretical knowledge. For the isonuclear sequence of iron ions, for example, a complete set of rate coefficients for electron-impact ionization and recombination has been constructed not too long ago by Arnaud and Raymond [5] from mostly theoretical calculations of cross sections and atomic structures of these ions including experimental results where available. Their tables are viewed as a prime source of information for plasma modelers.

The difficulty of establishing a consistent set of rate coefficients based on theoretical calculations alone can be demonstrated by comparing results presently available for dielectronic recombination (DR) of a relatively simple-structured ion: lithiumlike Fe^{23+}. Iron as an element and the Li-like system in particular is extremely important for plasma applications as well as for the basic understanding of electronic collision phenomena. Because of this importance numerous calculations of recombination rates have been carried out for DR involving the lowest core excited $2p$ and 3ℓ states of Fe^{23+}.

$$e + Fe^{23+}(1s^2 2s) \rightarrow Fe^{22+}(1s^2 n\ell n'\ell')$$

$$Fe^{22+}(1s^2 n\ell n'\ell') \rightarrow Fe^{22+}(1s^2 2s^2) + h\nu_1 + h\nu_2 \quad (1)$$

where $n = 2, 3$, $n' \geq n$ are the principal quantum numbers and ℓ, ℓ' the angular momentum quantum numbers of the intermediate excited sublevels populated by the two electrons which are active in the DR process. Results of different assessments of the rate coefficient for the process described by Eq. (1) are presented in Fig. 1. There is clearly a qualitative agreement of all the different approaches in that they predict a broad rate maximum around 10^5 K and a shoulder on that rate at about 5×10^6 K, where the $\Delta n \neq 0$ transitions become important. Rate coefficients for the temperature range relevant to the solar corona (at $T \approx 1$–2×10^6 K) are within an uncertainty bandwidth of a factor of more than 3 between the minimum and maximum predictions. At lower temperatures different calculations can differ from each other by any factor depending on the temperature of interest. Highly charged ions in such low temperature plasmas (kT in the low electron volt range) may

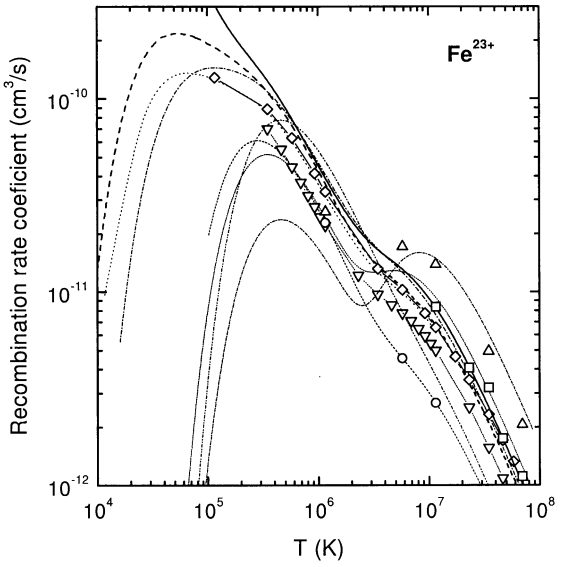

Fig. 1. Calculated plasma rate coefficients for dielectronic recombination of Fe^{23+} ($1s^2 2s$) ions: short dotted [6], dashed [7], dotted [8], dash-dotted [9], solid with diamonds [10], solid [5], short-dashed [11], short-dotted with down triangles [12], squares [13], circles [14], up triangles [15], short-dash-dotted [16], dot-dot-dashed [17]. Atomic structure data entering prescribed rate formulas were taken from the Oak Ridge "Redbook" [18], the rate coefficient referenced to Griffin and Pindzola [7] was calculated from their binned cross section data by Maxwellian convolution.

exist, for example in interstellar gas clouds when the plasma is driven by electromagnetic radiation from hot sources such as x-ray pulsars and x-ray binaries. For diagnosing such plasmas calculated rates for DR like those displayed in Fig. 1 are not of much help. It is most obvious that experiments are needed to test theoretical approaches and their predictive capabilities. And for particularly important cases, such as the iron sequence, experiments have to be performed to provide a reliable source of ionization and recombination cross section and rate data. Such experiments are now possible with highly charged ions at storage rings. As an example, rate coefficients for ionization and dielectronic recombination of Fe^{15+} ions are presented in this article.

2. The processes

The electron collision processes of general interest in this article involve multiply or highly charged atomic ions A^{q+} of a wide range of elements A. Two major categories of collisions are distinguished: (photo)recombination

$$e + A^{q+} \rightarrow \cdots \rightarrow A^{(q-1)+} + \text{photon(s)} \quad (2)$$

and net single ionization

$$e + A^{q+} \rightarrow \cdots \rightarrow A^{(q+1)+} + 2e \quad (3)$$

Both observation channels are characterized by the presence of direct and indirect mechanisms. The indirect reactions proceed via intermediate excited states indicated by the dots in Eqs. (2) and (3). Connections between ionization and recombination can be established by the observation of resonant intermediate excited states that decay to one or the other of these two observation channels.

Mechanisms of recombination, i.e. net production of $A^{(q-1)+}$ ions from A^{q+} ions, are as follows.

(1) Radiative recombination (RR)

$$e + A^{q+} \rightarrow A^{(q-1)+} + h\nu, \quad (4)$$

where the excess energy released by the binding of an initially unbound electron is carried away by a photon in a direct process. After radiative recombination the captured electron can be in a highly excited state and hence, further radiation will be emitted until the electron is in its ground level.

(2) Dielectronic recombination (DR) where, in a first step,

$$e + A^{q+} \rightarrow [A^{(q-1)+}]^{**} \quad (5)$$

the excess energy released by the capture of the electron is absorbed within the ion by the excitation of a core electron; and where, in a second step, the intermediate multiply excited state decays by the emission of two or more photons

$$[A^{(q-1)+}]^{**} \rightarrow [A^{(q-1)+}] + h\nu_1 + h\nu_2 \quad (6)$$

The first step of the DR process, the dielectronic capture [DC, Eq. (5)], can only occur if the kinetic energy E of the projectile electron matches the difference $E_{\text{res}} = E_i - E_f$ of total binding energies of all electrons in the initial and

final states of the ion. Its cross section can be described as

$$\sigma_{\mathrm{DC}}(E) = 7.88 \times 10^{-31}\ \mathrm{cm^2\ eV^2\ s}\ \frac{1}{E}\frac{g_f}{2g_i}\frac{A_a(f \to i)\Gamma}{(E - E_{\mathrm{res}})^2 + \Gamma^2/4} \quad (7)$$

where g_f and g_i denote the statistical weights of the state $|f\rangle$ formed by dc and of the initial state $|i\rangle$, respectively, $A_a(f \to i)$ is the autoionization rate of $|f\rangle$ for a transition to $|i\rangle$ and Γ the total width of $|f\rangle$. For the calculation of the cross section for DR σ_{DC} has to be multiplied by the fluorescence yield of the intermediate state $|f\rangle$.

(3) Three-body (or ternary) recombination (TR)

$$e + e + A^{q+} \to A^{(q-1)+} + e \quad (8)$$

where one of the two electrons can carry away the excess energy released by the recombination. TR becomes important at high electron densities and low energies, i.e. in a regime that is outside the scope of the present study.

Although not experimentally distinguished, the different recombination mechanisms lead to very characteristic energy dependences in the measured cross sections and rates. DR produces narrow resonances and can thus easily be identified in a measured recombination spectrum. The RR rate coefficient has its maximum at $E = E_{\mathrm{cm}} = 0$ eV and drops off as a smooth function of energy. Only in specific cases where RR and DR have identical initial and final states the two recombination mechanisms cannot be isolated. In that case interference effects may be observed.

Similarly, different ionization mechanisms leading to net production of $\mathrm{A}^{(q+1)+}$ from A^{q+} ions produce distinct features in the total cross section allowing the experimentalist to quantify individual contributions [19]. The most important single-ionization processes are as follows.

(1) Direct ionization (DI)

$$e + A^{q+} \to A^{(q+1)+} + 2e \quad (9)$$

proceeding in a single "knock-on" event.

(2) Excitation-autoionization (EA)

$$e + A^{q+} \to [A^{q+}]^{**} + e \quad (10)$$

$$[A^{q+}]^{**} \to A^{(q+1)+} + e \quad (11)$$

involving direct excitation of an inner-shell electron to a bound configuration of the A^{q+} ion and subsequent autoionization of the intermediate multiply excited $[A^{q+}]^{**}$ ion.

(3) Resonant-excitation-double autoionization (REDA)

$$e + A^{q+} \to [A^{(q-1)+}]^{**} \quad (12)$$

$$[A^{(q-1)+}]^{**} \to A^{(q+1)+} + 2e \quad (13)$$

involving a radiationless (dielectronic) capture of the incident electron by the A^{q+} ion and subsequent sequential emission of two electrons. REDA proceeds via intermediate compound states of the projectile electron and the parent ion and thus is closely related to the DR process [in fact, Eqs. (5) and (12) are identical].

Multiple ionization can also proceed via direct and indirect channels similar to the ones listed above for single ionization. In particular, inner-shell ionization with subsequent electron emission often contributes considerably to net multiple ionization of ions. For all resonant processes the cross section can be calculated by multiplying σ_{DC} [Eq. (7)] with the branching ratio for the particular decay path starting from the intermediate state $|f\rangle$.

3. Experimental issues

With their high energy resolution and, compared to bench-top measurements, high luminosity, storage ring merged-beam experiments are particularly well suited for detailed studies of electron–ion collisions. Among the available facilities, the heavy ion storage ring TSR of the Max-Planck Institute for Nuclear Physics in Heidelberg offers a number of advantages with respect to accessibility and beam intensity of ions with not too high charge states. Most of the plasma-relevant measurements carried out so far at

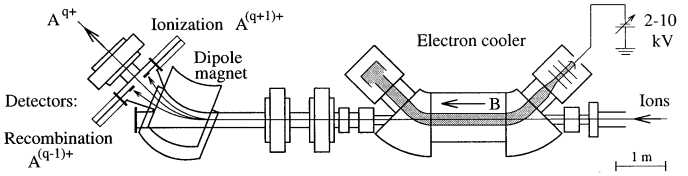

Fig. 2. Schematic of the cooler section of a storage ring (in this case the Heidelberg test storage ring TSR). The ion beam circulating in the ring is merged with the electron beam (shaded) of the electron cooler. Products of charge-changing collisions, i.e. ionized $A^{(q+1)+}$ and recombined $A^{(q-1)+}$ ions are separated from the beam of circulating A^{q+} ions by the dipole magnet behind the cooler and detected on the "inside" and "outside" of the ring, respectively.

storage rings have employed the TSR and this is also true for the examples presented in this article.

For the measurement of rates and cross sections ions of the desired species are injected into the ring from an accelerator. High beam currents up to the milliamp range can be accumulated depending on the ion species. The ions are cooled by the interaction with the electron beam of the cooling device (see Fig. 2). So far, this beam has to serve both for the cooling of ion beams and as an electron target for collision experiments. By the implementation of an electron target in addition to the cooler, future experiments will profit from easier beam handling, still better energy resolution and a wider range of accessible electron–ion center-of-mass energies.

When the ion beam is sufficiently cold the energy of the electron beam is detuned from "cooling" and accordingly, the relative energy between the ion and electron beams is increased from zero. In the collisions with electrons of the cooler, stored ions change their original charge state and, by that, drop out of the ring and can be detected without disturbing the circulating ion beam. Suitable particle detectors are mounted both at the outer and the inner side of the ring, typically behind the first beam-bending magnet downbeam from the electron cooling device (see Fig. 2) such as to facilitate collection of recombined and ionized product ions, respectively. Counting rates R_{exp} are recorded as a function of the electron energy which is rapidly scanned over a certain range usually in small steps with intermittend beam cooling after each voltage step.

Normalized collision rates α are determined from the relation

$$\alpha(E_{\mathrm{rel}}) = \frac{R_{\mathrm{exp}}\gamma^2 v_i qe}{I_i \ell_{\mathrm{eff}} n_e \epsilon} \tag{14}$$

Detection efficiencies ϵ of the particle detectors are usually close to 1, I_i is the measured electrical current of the circulating ion beam, v_i the ion velocity (in the laboratory frame), qe the ion charge, l_{eff} the interaction length of the two beams, n_e the electron density, and $\gamma = \gamma(v_i)$ the relativistic Lorentz factor for the ion beam in the laboratory frame. The rates α basically depend on the velocity spread within the electron beam and the collision cross section σ:

$$\alpha(v_{\mathrm{rel}}) = \langle \sigma v_{\mathrm{rel}} \rangle = \int \sigma(v) v f(v_{\mathrm{rel}}, \mathbf{v})\, d^3v \tag{15}$$

For the particular case of merged electron and ion beams in storage cooler rings, two velocity coordinates are commonly used to describe the electron-velocity distribution in the rest frame of the ions: $v_{\|}$, the velocity component in electron-beam direction, and $v_{\perp}$, the velocity component perpendicular to the electron-beam direction. The energy (or velocity) spreads are therefore characterized by two corresponding temperatures $T_{\|}$ for the longitudinal and $T_{\perp}$ for the transverse direction. In the accelerated electron beam, these temperatures are quite different with $T_{\|} \ll T_{\perp}$, so that $f(\mathbf{v})$ is highly anisotropic. Its mathematical form is given by

$$f(v_{\mathrm{rel}}, \mathbf{v}) = \frac{m_e}{2\pi k T_{\perp}} \exp\left(-\frac{m_e v_{\perp}^2}{2kT_{\perp}}\right) \sqrt{\frac{m_e}{2\pi k T_{\|}}} \times \exp\left(-\frac{m_e (v_{\|} - v_{\mathrm{rel}})^2}{2kT_{\|}}\right) \tag{16}$$

where m_e denotes the electron rest mass. The quantity v_{rel} in this formula is the average longitudinal electron velocity in the rest frame of the ion

$$v_{\mathrm{rel}} = \frac{|v_{e,\|} - v_{i,\|}|}{1 + (v_{i,\|} v_{e,\|}/c^2)}, \tag{17}$$

where c is the vacuum speed of light, and where $v_{e,\|}$ and $v_{i,\|}$ are the longitudinal velocity components of the electron and ion beams in the laboratory frame, respectively. They are determined from

$$v_{e,\|} = c\sqrt{1 - [1 + (E_e/m_e c^2)]^{-2}} \tag{18}$$

and

$$v_{i,\|} = c\sqrt{1 - [1 + (E_i/m_i c^2)]^{-2}} \tag{19}$$

The ion rest mass is represented by m_i. The energies E_e and E_i are determined by electron and ion acceleration voltages, respectively. The relative velocity v_{rel}, as defined by Eq. (17), is principally different from the velocity v_{cm} in the electron–ion center-of-mass frame. Assuming negligible transverse velocity components in the ion beam the center-of-mass velocity can be represented by

$$v_{\mathrm{cm}} = \sqrt{(v_{\mathrm{rel}} \pm v_{\|})^2 + v_{\perp}^2} \tag{20}$$

where $v_{\|}$ and $v_{\perp}$ are distributed according to Eq. (16) at given temperatures $T_{\|}$ and $T_{\perp}$. The difference between v_{cm} and v_{rel} is relevant only for low energies, where $E = E_{\mathrm{cm}}$ comes close to $kT_{\perp}$ and $kT_{\|}$. There the perpendicular velocity components $v_{\perp}$ (being of the magnitude of $kT_{\perp}/m_e \approx 10^5$ m/s) can make a significant contribution to the size of v_{cm}. Since only E_{rel} is directly accessible to a measurement, experimental data are usually displayed as a function of the relative energy

$$E_{\mathrm{rel}} = (\gamma_{\mathrm{rel}} - 1) m_e c^2 \tag{21}$$

with

$$\gamma_{\mathrm{rel}} = [1 - (v_{\mathrm{rel}}/c)^2]^{-1/2} \tag{22}$$

The statistical occurrence of velocity components $v_{\|}$ and $v_{\perp}$ in Eq. (20) results in an energy spread and hence, determines the energy resolution r of the measurement

$$r = \frac{E_{\mathrm{rel}}}{\Delta E} = \frac{E_{\mathrm{rel}}}{\sqrt{(kT_{\perp} \ln 2)^2 + 16 E_{\mathrm{rel}} kT_{\|} \ln 2}} \tag{23}$$

With electron beams adiabatically expanded in a decreasing magnetic field temperatures $kT_{\perp}$ in the vicinity of 1 meV are accessible. Careful acceleration of the electron beam results in longitudinal temperatures that can be as low as roughly 0.1 meV. Thus the energy resolution in a storage ring experiment at $E_{\mathrm{rel}} = 1000$ eV can be as high as $r = 1000$.

When $E_{\mathrm{rel}} \gg kT_{\perp}$, $kT_{\|}$ the velocity v_{rel} approaches v_{cm} and hence Eq. (15) can be rewritten as

$$\alpha(v_{\mathrm{rel}}) \approx v_{\mathrm{rel}} \int \sigma(v)\, f(v_{\mathrm{rel}}, \mathbf{v})\, d^3v = v_{\mathrm{rel}} \sigma_{\mathrm{app}} \tag{24}$$

The apparent cross section σ_{app} results from the convolution of the real cross section σ with the experimental velocity (or energy) distribution. This quantity makes physical sense when the width of the distribution function is much smaller than v_{rel} (or E_{rel}, respectively). In this case, apparent cross sections

$$\sigma_{\mathrm{app}} = \alpha(v_{\mathrm{rel}})/v_{\mathrm{rel}} \tag{25}$$

are used instead of rate coefficients α.

Particularly in recombination experiments, the measured rates and cross sections are modified by field ionization of Rydberg states in the beam-bending magnets. For applications in plasma physics, this truncation of the Rydberg state distribution has to be considered. Statistical uncertainties of the measured data can in most cases be reduced to insignificance, total systematic uncertainties are typically of the order of $\pm 20\%$.

The formalism described by Eqs. (15) and (16) is a generalization of what is needed to determine plasma rate coefficients $\alpha(T)$ from the measurements performed at storage rings

$$\alpha(T) = (kT)^{-3/2} \sqrt{\frac{8}{m\pi}} \int_0^{\infty} \sigma(E)\, E \exp\left(-\frac{E}{kT}\right) dE \tag{26}$$

Different from the situation in merged beams experiments the plasma temperature T is assumed to be isotropic. The parameter m is the reduced mass of the electron–ion collision system and as such is very close to m_e.

In the storage ring measurements the ensembles of colliding particles, the electrons and ions, have a well defined average relative velocity v_{rel}. As a consequence, high resolution is obtained in the whole range of accessible energies and hence, cross sections can be measured in great detail. In contrast to that, convolution of the measured data following Eq. (26) leads to broad smooth dependences of plasma rate coefficients $\alpha(T)$, where most of the details in the cross sections are washed out. Nevertheless, the details of the cross sections at low energies have a strong influence on the size of plasma rate coefficients at low temperatures.

4. Results for Fe^{15+} ions

The difficulties of theory-based determination of plasma rate coefficients are highlighted by an investigation of Na-like $Fe^{15+}(1s^22s^22p^63s)$. The potential of storage ring measurements can be well demonstrated by this example.

4.1. Electron-impact net single ionization

Ionization cross sections of Li-like Si^{11+} and Cl^{14+} [20], as well as of Na-like Cl^{6+}, Fe^{15+}, and Se^{23+} [21,22] have been measured at the TSR. The lower-charge Na-like ions are already in the feasibility range of modern ion sources which deliver sufficiently intense beams at the favorable low energies where electron stripping and hence also production of background in the residual gas is greatly suppressed. Nevertheless, even for these ions the storage rings offer a decisive advantage: In the hot plasmas of ion sources producing highly charged ions, usually large amounts of ions in excited states are generated. Many of these states live sufficiently long to reach the electron–ion interaction region and thus cause severe normalization problems due to unknown fractions of different excitation stages in the parent ion beam. An additional complication had to be faced in previous ionization experiments with Na-like ions. The parent beams contain metastable autoionizing states which produce huge background signals when decaying in the interaction path. In a storage ring experiment, however, storage of the ions for only a few seconds make the metastable states completely go away and then the measurement can start without that background and with a parent beam where all ions are in their ground state.

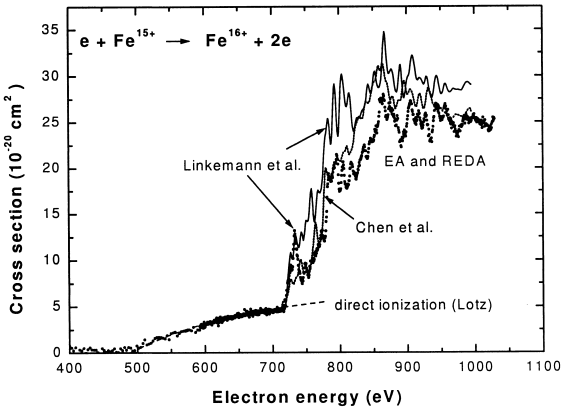

Fig. 3. Cross sections for electron-impact ionization of Fe^{15+} ions. The experimental data [22] are indicated by solid circles. The solid and dotted lines are the results of extensive theoretical calculations [22,23]. Direct ionization was estimated using the semi-empirical formula introduced by Lotz [24].

As an example for the results obtained at the TSR in Heidelberg, Fig. 3 shows the measured cross sections for electron-impact single ionization of Fe^{15+} ions in an energy range from below threshold up to about 1 keV. The experimental data are displayed together with two theoretical calculations. Above 750 eV the cross section is dominated by indirect processes EA and REDA (see Sec. 2). Particularly remarkable is the wealth of resonance features which are due to resonant electron capture DC and subsequent emission of two electrons. Although theory reproduces the overall size and structure of the measured cross section, the fine details observed in the experiments are not matched by the calculations.

For the determination of the plasma rate coefficient for electron-impact single ionization of Fe^{15+} the

measured cross section function has to be convoluted according to Eq. (26) with isotropic temperature-dependent Maxwellians [Eq. (16), $v_{rel} = 0$, $T = T_\perp = T_\parallel$]. For each temperature the distribution has to be integrated over the complete energy range from 0 to ∞, which in principle requires knowledge of the cross section at any given energy. For most practical purposes, however, energies $E \gg kT$ do not contribute much to $\alpha(T)$. For ions as highly charged as Fe^{15+}, however, temperatures up to the kiloelectron volt range are of practical interest. In this respect, the measurements displayed in Fig. 3 are not sufficient to determine reliable plasma rate coefficients for temperatures beyond $kT \approx 100$ eV. A reasonable extrapolation of the measured data towards higher energies is necessary before $\alpha(T)$ can be calculated over the desirable range of temperatures.

In the case of Fe^{15+} the ionization cross section is characterized by DI of the M and L shells (ionization of the K shell can be neglected at the energies of interest here), by excitation of the L shell and subsequent autoionization (EA) and by resonant L-shell excitation with subsequent double autoionization (REDA). DI of a given subshell (index ν) can be rather well represented by the Lotz formula [24]

$$\sigma_\nu = 4.5 \times 10^{-14}\ \mathrm{cm^2\ eV^2}\ \frac{\xi_\nu}{I_\nu E} \ln \frac{E}{I_\nu}, \qquad (27)$$

where ξ_ν is the number of equivalent electrons in the νth subshell, I_ν the ionization potential of that subshell, and E the electron energy. The applicability of Eq. (27) is demonstrated in Fig. 3 where the Lotz formula apparently describes the low energy DI part of the ionization cross section for Fe^{15+} very well. Equation (27) can be easily evaluated for higher energies and reasonable results can be expected as long as the energies are nonrelativistic.

The region of significant REDA contributions has been covered rather completely by the experiment, an extrapolation of that part of the cross section is not necessary. The EA process involves excitation of a large number of doubly excited states and the cross section for those cannot easily be predicted. However, since the experimental cross section covers the excitation thresholds of all the states which can be expected to contribute, the extrapolation just requires the knowledge of the cross-section energy dependence beyond $E = 1$ keV. The related function can then be normalized to the experiment at the EA threshold. Cross sections for direct excitation can be approximated for example by the Gaunt-factor formula of Seaton [25] and van Regemorter [26]

$$\sigma = 2.36 \times 10^{-13}\ \mathrm{cm^2\ eV^2}\ \frac{f_{ij}\bar{g}}{EE_{ij}}, \qquad (28)$$

where f_{ij} is the oscillator strength for the transition from excited state j to ground state i, E_{ij} the related excitation energy, E the electron energy, and $\bar{g}$ the effective Gaunt factor. Near threshold this is reasonably well approximated by $\bar{g} = 0.2$. At higher energies, the recommendation is

$$\bar{g} = 0.28 \ln (E/E_{ij}) \qquad (29)$$

For the present extrapolation, a single (averaged) excitation threshold $E_{ij} = 800$ eV was used and smooth convergence assumed of $\bar{g}$ from 0.2 to the function represented by Eq. (29). The oscillator strength together with the branching ratio for the autoionization subsequent to L-shell excitation [in other words, the constant factor in Eq. (28)] was adjusted such that the experiment was matched by the sum of the constructed cross sections for DI and EA in the vicinity of $E = 1000$ eV. The extrapolated and measured cross sections are shown in Fig 4. The resulting data have then been used to infer the plasma rate coefficient for ionization by employing Eq. (26). The result is shown in Fig. 5 and compared with the data recommended by Arnaud and Raymond [5] as well as the rate coefficient determined on the basis of cross section measurements by Gregory et al. [27]. Up to temperatures of about 10^7 K all three data sets are in rather good agreement. Beyond that temperature the uncertainties of the extrapolation of experimental cross sections cause discrepancies between the different data sets. Apparently, the ionization rate coefficients determined by Arnaud and Raymond for Fe^{15+} ions are pretty much confirmed by the experiments below 10^7 K if a 20% difference is accepted. Beyond

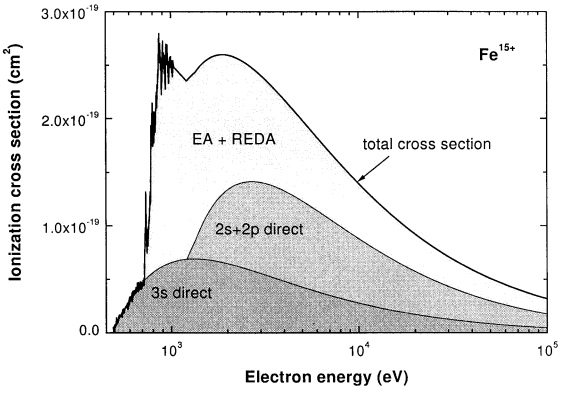

Fig. 4. Measured and extrapolated cross sections for electron-impact ionization of Fe^{15+} ions. The experimental data [22] are from Fig. 3. The cross section for energies beyond 1050 eV has been inferred from the sum of the direct ionization contributions from the *L* and *K* shells using the Lotz formula [24] and an EA contribution with an energy dependence as predicted by the Gaunt-factor formula [25,26]. The different calculated contributions are indicated by differently shaded areas.

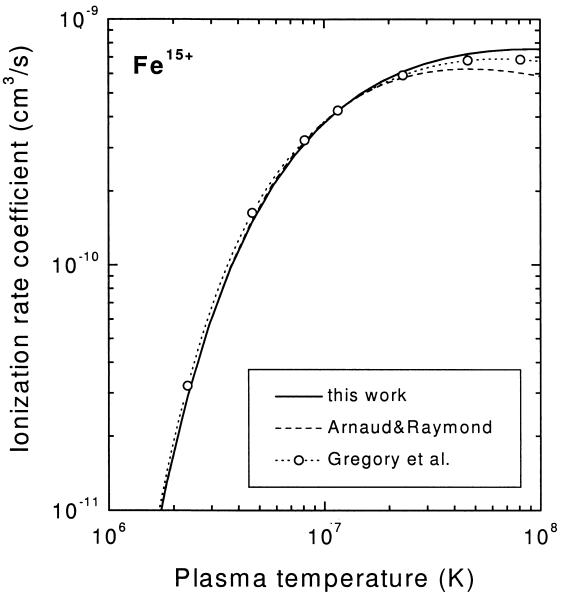

Fig. 5. Maxwellian plasma rate coefficients for electron-impact single ionization of Fe^{15+} ions. The present data were determined from the cross sections given in Fig. 4 by convolution with a Maxwell-Boltzmann distribution according to Eq. (26). The result is compared with the data recommended by Arnaud and Raymond [5] and the rate coefficients calculated from the experimental data of Gregory et al. [27]. The three data sets are in fairly good agreement at temperatures below 10^7 K. At higher temperatures the differences in the three curves just reflect the uncertainty of the cross section extrapolation beyond 1 keV.

10^7 K the lack of a real experimental basis forbids further conclusions on the recommended theoretical data.

4.2. Dielectronic recombination

Recombination measurements with ions in intermediate high charge states are relatively straightforward at storage rings. Most ions present in the solar corona or in a fusion plasma can easily be studied for example at the TSR.

The expected high quality of x-ray spectra from astrophysical objects to be obtained in future satellite experiments has led to a research program at the TSR in which recombination (and partly also ionization—see the previous chapter) of the cosmically abundant ions Fe^{q+} with $q = 15, 16, \ldots, 23$ is being studied. Recently, the measurement of the recombination spectrum of fluorine like Fe^{17+} ions provided a surprise for the astrophysics community [28]. Different from all previous expectations the experiment showed the importance of M1 excitations of the $^2P_{3/2}$ core of Fe^{17+} ions in DR. Hence, in the cold plasma of x-ray driven interstellar nebulae, the DR rate coefficient can be much higher (by two orders of magnitude) than previous results that are based on calculations considering only pure LS coupling. Experimental data are also available at this time for Fe^{18+}, and measurements with Fe^{19+} ions have recently been successfully completed. The results are presently being prepared for publication.

The most detailed set of measurements in the iron isonuclear sequence is available for Fe^{15+} ions [21], where recombination was studied in an energy range from zero to more than 1000 eV covering resonances due to core transitions from $3s$ to $3\ell'$, $4\ell'$ and higher, as well as from 2ℓ to $3\ell'$, $4\ell'$ and higher. The rate data are obtained with extremely high energy resolution particularly at the very low energies. Energy spreads ΔE as low as 10 meV have been observed in storage ring experiments. This allows for the observation of the very rich structure in the recombination

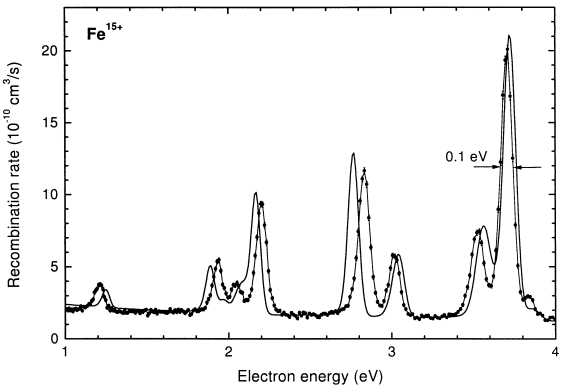

Fig. 6. Measured and calculated dielectronic recombination rates [21] of Fe^{15+} ions in a narrow electron energy range. The resonances are associated with configurations $1s^22s^22p^63p_{1/2}10\ell$ and $1s^22s^22p^64\ell4\ell'$.

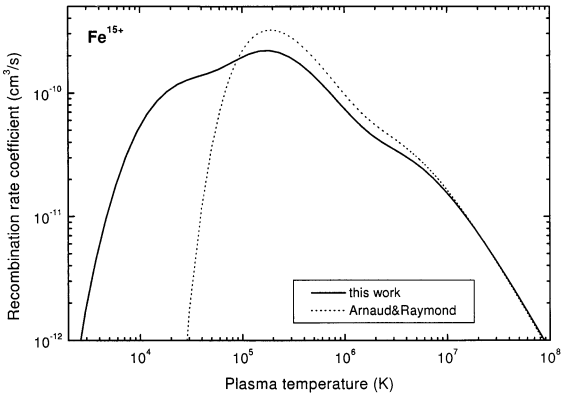

Fig. 7. Maxwellian plasma rate coefficients for dielectronic recombination of Fe^{15+} ions with electrons. The present data (solid line) were determined from the measurements of Linkemann et al. [21] which cover the complete energy range from 0 to 1050 eV. The dashed line represents the recommended rate coefficient determined by Arnaud and Raymond [5].

(and ionization) rates and cross sections as demonstrated for the ionization channel already by Fig. 3.

An example for recombination measurements is shown in Fig. 6. The total recombination rate, i.e. the sum of radiative and dielectronic recombination (RR + DR) rates, is shown as a function of $E = E_{\mathrm{rel}}$, the electron–ion relative energy, in a range of only 3 eV. Already in this narrow energy range there are a number of narrow resonances observed with peak widths of the order of 0.1 eV. These resonances are associated with doubly excited intermediate configurations $1s^22s^22p^63p_{1/2}10\ell$ and $1s^22s^22p^64\ell4\ell'$. Also shown in Fig. 6 is a theoretical calculation [21]. The calculated rate is in almost perfect agreement with the experiment. A closer look, however, reveals shifts in the resonance energies and differences in peak areas. Apparently it is difficult to predict resonance positions with uncertainties lower than a few tenths of an electron volt, even with the most advanced theoretical approaches to DR. This difficulty of theory to calculate exact resonance positions has been a source of huge uncertainties in plasma rate coefficients at low temperatures ($kT \lessapprox 10^5$ K). Fig. 1 provides vivid testimony of this situation. For Fe^{15+} the present theory does reproduce the experimental resonance energies rather well. This may be a consequence of the relatively simple atomic structure of that ion with only one electron in the M shell outside closed K and L shells. It is certainly also due to the relatively advanced theoretical approach used in the calculation that is shown in Fig. 6.

The experimental plasma rate coefficients displayed in Fig. 7 were deduced from the recombination measurements [21] mentioned above. The contribution of radiative recombination was subtracted from the measured data by representing the RR rate by a smooth curve with an appropriate $1/\sqrt{E}$ dependence such that the resulting DR rate between fully resolved resonance peaks is zero. Since the measurements covered the full energy range for M- and L-shell core excitations no extrapolation is necessary this time to calculate the total plasma rate coefficients. The contribution of K-shell excited resonances can be neglected in the temperature range presented in Fig. 7.

The comparison of the experimental and the recommended plasma rate coefficient data clearly reveals again the issue about resonance energies discussed above (see Fig. 7). At low temperatures where the plasma rates sensitively depend on the DR resonance positions there is no agreement at all between the present results and the data of Arnaud and Raymond [5], which are preferably used in plasma modeling calculations. Apparently, the low-energy DR resonances have not properly been accounted for in the

theoretical plasma rate assessment. Above temperatures corresponding to $kT \lessapprox 10^5$ K the two data sets approach each other to within the 50% level and beyond 10^7 K can hardly be distinguished from each other.

Both the data of Arnaud and Raymond and the results of this work show a shoulder in the plasma rate curve at about 3×10^6 K. This structure is due to contributions from L-shell excited core states with associated Rydberg series of resonances. The maximum at about 2×10^5 K of the plasma rate is mainly due to high Rydberg states associated with $3s \rightarrow 3\ell$ and $3s \rightarrow 4\ell$ core transitions. The experimental rates reveal an additional structure at about 3×10^4 K which is not reproduced by the results obtained by Arnaud and Raymond. The bump is due to the lowest DR resonances as the ones displayed in Fig. 6. In many theoretical papers these low temperatures were excluded from the calculation of plasma rates because of the difficulties of calculating the resonance energies sufficiently well. The resonance energy in turn has a strong influence on the strength of the resonance if it is located at low energies. There, the relative uncertainty of the calculated energy can easily be several hundred percent, and, since the DR cross section involves a $1/E$ factor [apart from the Lorentzian resonance shape, see Eq. (7)] the size of a resonance can be off also by several hundred percent.

For most purposes in connection with stellar atmospheres like the solar corona, these very low temperatures are of minor importance in connection with highly charged ions. Arnaud and Raymond [5] predict peak abundance of Fe^{15+} in a (thermal) coronal equilibrium plasma at temperatures of about 2×10^6 K far above the temperatures where the discrepancies between the present data and the recommended plasma rate coefficients occur. However, there are plasma environments such as x-ray driven interstellar nebulae where highly charged ions, e.g. Fe^{15+}, Fe^{16+}, and so forth up to Fe^{23+}, are produced by photoionization and the plasma temperature is only in the electron volt range. In such photoionized gases low-energy recombination plays a most important role and determines the nature of the emitted radiation. There it is essential to know the exact positions and strengths of DR resonances in order to perform reasonable plasma modeling. Such information can be obtained now experimentally at heavy ion storage rings for almost all plasma-relevant ion species. The experimental techniques have been well developed during the last decade and the measurements are precise and relatively straightforward.

Yet, there is another additional serious complication in the determination of realistic plasma rate coefficients for electron–ion recombination, which calls the presently used plasma rates in question even more than the previous considerations.

It has been recognized early by Burgess and Summers [29] and Jacobs et al. [30] that dielectronic recombination in the presence of an electric field (DRF) is qualitatively and quantitatively different from DR in a field free environment. Clear evidence that DR cross sections depend on the presence and size of external electromagnetic fields in the collision region has been found in a number of experiments [31–33]. These measurements were carried out with controlled external electric and magnetic fields and have revealed substantial cross section enhancement factors for high Rydberg states. Theoretical techniques have been developed to account for electric fields and their influence on DR [34]. Calculations using the DRFEUD package of Griffin et al. [35] have been in reasonable overall agreement with available experimental observations [36–39]. In the details, however, there are discrepancies between theory and experiment [33] which have been attributed recently to the combined effects of crossed electric and magnetic fields [40–42]. Such fields are ubiquitous in any kind of plasma and hence, field effects definitely have to be considered when recombination rates are determined for plasma modeling.

So far, there is no experimental result available concerning field effects on DR for Fe^{15+}, however, a comparison of theoretical DR calculations with and without electric fields has been published previously by Griffin and Pindzola [7] for this very ion. The calculation includes Rydberg states with principal quantum numbers up to 100 and $\Delta n = 0$ and $\Delta n = 1$ core transitions starting from the $3s$ subshell. The maximum electric field was chosen to be 10 kV/cm

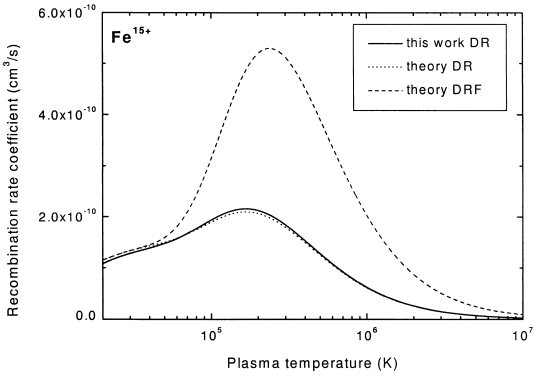

Fig. 8. Influence of an external electric field on plasma rate coefficients for recombination of Fe^{15+} ions with electrons. The rate coefficients are for dielectronic recombination processes involving $3s \rightarrow 3\ell$ and $3s \rightarrow 4\ell$ core excitations in the energy range 0–40 eV only. The solid line was calculated by convolution [according to Eq. (26)] of the experimental results of Linkemann et al. [21] restricted to the energy interval mentioned previously. These data were taken with no or at most little external field (<10 V/cm) in the collision region. The theoretical curves were obtained by convoluting the cross sections published by Griffin and Pindzola [7] for zero field and for a field of 10 kV/cm, respectively, where for the latter saturation of the field enhancement was expected. The calculations were limited to Rydberg states up to $n = 100$. The experimental data are truncated by a field-ionization cutoff at about the same principal quantum number.

assuming that electric field enhancement of DR is saturated at this field strength. In the energy region right below the series limits of $3\ell n\ell'$ Rydberg states, i.e. at about 34 and 37 eV the field enhancement of the cross section is roughly as high as an order of magnitude. The convolution of the calculated DR cross sections with and without field using Eq. (26) produces the dashed and dotted curves in Fig. 8. The plasma rate coefficients presented in Fig. 8 are partial in the sense that only DR resonances up to 40 eV were included in the convolution. The same restriction was applied to the convolution of the experimental DR cross section of Linkemann et al. [21]. For the field free case theory can be compared with experiment. The agreement in the investigated temperature range is truly remarkable. According to the present state of our knowledge the calculation of the rate coefficient in the presence of a strong electric field can be expected to give a reasonable result as well. At temperatures typical for the solar corona the plasma rate coefficient from the DRF calculation is about a factor of 4 above the normal DR rate calculated without inclusion of fields.

5. Summary and outlook

The comparisons of plasma rate coefficients determined theoretically or by experiments clearly reveal the need for a better data basis than it is presently available. Although there appears to be quite reasonable agreement between recommended plasma rates for electron-impact ionization published by Arnaud and Raymond [5] with the present experimental findings this agreement may partially be fortuitous. These authors could already compare their predictions for the ionization of Fe^{15+} with an available experiment by Gregory et al. [27] as well as a very advanced theoretical calculation by Chen et al. [23] and they found satisfactory agreement within the existing uncertainties of the experimental result. There are other ion species with an even simpler electronic structure than Fe^{15+} where the experimental and theoretical ionization cross sections cannot be made to agree with each other. An example for that is the ionization of Be^{+} ions [43,44] where the experiments are about a factor 1.5 above the theory even for DI only. Discrepancies of 50% and more between experiments and advanced calculations which treat all possible direct and indirect processes have always to be expected in total single ionization cross sections. Differences in partial cross sections for specific EA or REDA or still higher-order processes may be as much as a factor of 10.

The situation concerning dielectronic recombination of ions is apparently even more severe. Serious discrepancies exist between different theoretical predictions of DR plasma rate coefficients particularly at rather low temperatures, however, theoretical uncertainties of as much as a factor 3–5 have been revealed in our studies at storage rings even at temperatures relevant for the solar corona [28]. With the representative example of Fe^{15+} ions in this article the main problems in accurately predicting plasma rate coefficients have been documented. An additional problem

enters through the dependence of dielectronic recombination on the presence and size of external electromagnetic fields. Although the influence of electric fields seemed to be fairly well understood, recent experimental findings and new theoretical approaches indicate an additional influence of magnetic fields when they occur in combination with perpendicular electric field components. Detailed calculations of total DRF cross sections taking into account both, electric and magnetic fields would require an enormous logistic and computational effort and are presently not possible. First experiments are providing quantitative results, however, the experimental parameter range presently accessible is somewhat restricted. The necessary magnetic guiding fields for the electron beam in electron coolers at storage rings are at least about 0.02 T. The combination of electric fields with magnetic fields 10–100 times less would be desirable to test upcoming theoretical predictions.

As the examples in this article show, storage rings have opened up vast possibilities to study plasma-relevant collisions of highly charged ions and presently, data with excellent quality are becoming available. Much more work and developments both in theory and experimental techniques will be necessary to solve the existing problems with the prediction of reliable plasma rate coefficients for highly charged ions in the presence of external fields.

Acknowledgements

The author gratefully acknowledges the fruitful collaboration of his research group in Giessen with the atomic physics group at the TSR in Heidelberg. Work of previous members of the groups, J. Linkemann and J. Kenntner, was essential for the assessment of the present data material. Fruitful discussions and scientific interaction with S. Schippers, A. Wolf, and D. Savin on the present subject is gratefully acknowledged. This work is supported by the German Federal Government through contract nos. BMBF 06 GI 848 and 06 HD 854.

References

[1] Atomic Processes, in Electron–Ion and Ion–Ion Collisions, F. Brouillard (Ed.), Plenum, New York, 1986.
[2] Recombination of Atomic Ions, NATO ASI Series B: Physics Vol. 296, W.G. Graham, W. Fritsch, Y. Hahn, J.H. Tanis (Eds.), Plenum, New York, 1992.
[3] A. Müller, A. Wolf, in Accelerator-Based Atomic Physics Techniques and Applications, S. Shafroth, J. Austin (Eds.), American Institute of Physics, Woodbury, NY, 1997, Chap. 5, pp. 147–182.
[4] A. Müller, T. Bartsch, C. Brandau, A. Hoffknecht, H. Knopp, S. Schippers, O. Uwira, J. Linkemann, A.A. Saghiri, M. Schmitt, D. Schwalm, A. Wolf, F. Bosch, B. Franzke, C. Kozhuharov, P.H. Mokler, F. Nolden, M. Steck, T. Stöhlker, T. Winkler, H. Danared, D.R. DeWitt, H. Gao, H. Lebius, R. Schuch, W. Spies, W. Zong, G. Dunn, W.G. Graham, J.A. Tanis, J. Doerfert, D.W. Savin, Z. Stachura, Proceedings of the Third Euroconference on Atomic Physics with Stored Highly Charged Ions, Ferrara, Italy, 22–26 September 1997, Hyperfine Interactions 114 (1998) 229–235.
[5] M. Arnaud, J. Raymond, Astrophys. J. 398 (1992) 394–406.
[6] A. Burgess, Ap. J. 141 (1965) 1588–1590.
[7] D.C. Griffin, M.S. Pindzola, Phys. Rev. A 35 (1987) 2821–2831.
[8] K. Moribayashi, T. Kato, National Institute for Fusion Science, Research Report no. NIFS-DATA-41, Nagoya, Japan, 1997.
[9] C.J. Romanik, Astrophys. J. 330 (1988) 1022–1035.
[10] M.H. Chen, Phys. Rev. A 44 (1991) 4215–4223.
[11] D.T. Woods, J.M. Shull, C.L. Sarazin, Ap. J. 249 (1981) 399–401.
[12] L.J. Roszman, Phys. Rev. A 35 (1987) 2122–2137.
[13] D.J. McLaughlin, Y. Hahn, J. Quant. Spectrosc. Radiat. Transfer 28 (1982) 343–353; Phys. Rev. A 29 (1984) 712–720.
[14] V.L. Jacobs, J. Davis, P.C. Kepple, M. Blaha, Astrophys. J. 211 (1977) 605.
[15] H.P. Summers, Mon. Not. R. Astron. Soc. 158 (1972) 255; 169 (1974) 663.
[16] V.P. Zhdanov, Sov. Phys. JETP 48 (1978) 611–615; J. Phys. B: At. Mol. Phys. 15 (1982) L541–L544.
[17] I.L. Beigman, L.A. Vainshtein, B.N. Chichkov, Sov. Phys. JETP 53 (1981) 490–494.
[18] Spectroscopy Data for Iron, W.L. Wiese (Ed.), in ORNL-6089/V4 Atomic Data for Controlled Fusion Research, Vol. IV, Controlled Fusion Atomic Data Center, Oak Ridge National Laboratory, Oak Ridge, 1985.
[19] A. Müller, in Physics of Ion Impact Phenomena, D. Mathur (Ed.), Springer, Berlin, 1991, pp. 13–90.
[20] J. Kenntner, J. Linkemann, N.R. Badnell, C. Broude, D. Habs, G. Hofmann, A. Müller, M.S. Pindzola, E. Salzborn, D. Schwalm, A. Wolf, Seventh International Conference on the Physics of Highly Charged Ions, Vienna, Austria, 19–23 September 1994, Nucl. Instrum. Methods Phys. Res. B 98 (1995) 142–145.
[21] J. Linkemann, J. Kenntner, A. Müller, A. Wolf, D. Habs, D.

Schwalm, W. Spies, O. Uwira, A. Frank, A. Liedtke, G. Hofmann, E. Salzborn, N.R. Badnell, M.S. Pindzola, Seventh International Conference on the Physics of Highly Charged Ions, Vienna, Austria, 19–23 September 1994, Nucl. Instrum. Methods Phys. Res. B 98 (1995) 154–157.
[22] J. Linkemann, A. Müller, J. Kenntner, D. Habs, D. Schwalm, A. Wolf, N.R. Badnell, M.S. Pindzola, Phys. Rev. Lett. 74 (1995) 4173–4176.
[23] M.H. Chen, K.J. Reed, D.L. Moores, Phys. Rev. Lett. 64 (1990) 1350–1353.
[24] W. Lotz, Z. Phys. 216 (1968) 241.
[25] M.J. Seaton, The theory of excitation and ionization by electron impact, in Atomic and Molecular Processes, D.R. Bates (Ed.), Academic, New York, 1962, p. 374.
[26] H. Van Regemorter, Astrophys. J. 136 (1962) 906.
[27] D.C. Gregory, L.-J. Wang, F.W. Meyer, K. Rinn, Phys. Rev. A 35 (1987) 3256.
[28] D.W. Savin, T. Bartsch, M.H. Chen, S.M. Kahn, D.A. Liedahl, J. Linkemann, A. Müller, M. Schmitt, D. Schwalm, A. Wolf, Astrophys. J. Lett. 489 (1997) L115–L118.
[29] A. Burgess, H.P. Summers, Astrophys. J. 157 (1969) 1007.
[30] V.L. Jacobs, J. Davis, P.C. Kepple, Phys. Rev. Lett. 37 (1976) 1390; V.L. Jacobs, J. Davis, Phys. Rev. A 19 (1979) 776.
[31] A. Müller, D.S. Belić, B.D. De Paola, N. Djurić, G.H. Dunn, D.W. Mueller, C. Timmer, Phys. Rev. Lett. 56 (1986) 127–130; Phys. Rev. A 36 (1987) 599–613.
[32] A.R. Young, L.D. Gardner, D.W. Savin, G.P. Lafyatis, A. Chutjian, S. Bliman, J.L. Kohl, Phys. Rev. A 49 (1994) 357–362; D.W. Savin, L.D. Gardner, D.B. Reisenfeld, A.R. Young, J.L. Kohl, ibid. 53 (1996) 280–289.
[33] T. Bartsch, A. Müller, W. Spies, J. Linkemann, H. Danared, D.R. De Witt, H. Gao, W. Zong, R. Schuch, A. Wolf, G.H. Dunn, M.S. Pindzola, D.C. Griffin, Phys. Rev. Lett. 79 (1997) 2233–2236.
[34] Y. Hahn, Rep. Prog. Phys. 60 (1997) 691–759.
[35] D.C. Griffin, M.S. Pindzola, C. Bottcher, Phys. Rev. A 33 (1986) 3124.
[36] P.F. Dittner, S. Datz, in [2], p. 133.
[37] L.H. Andersen, J. Bolko, P. Kvistgaard, Phys. Rev. A 41 (1990) 1293–1302.
[38] L.H. Andersen, G.-Y. Pan, H.T. Schmidt, M.S. Pindzola, N.R. Badnell, Phys. Rev. A 45 (1992) 6332–6338.
[39] S. Schennach, A. Müller, O. Uwira, J. Haselbauer, W. Spies, A. Frank, M. Wagner, R. Becker, M. Kleinod, E. Jennewein, N. Angert, P.H. Mokler, N.R. Badnell, M.S. Pindzola, Z. Phys. D 30 (1994) 291–306.
[40] F. Robicheaux, M.S. Pindzola, Phys. Rev. Lett. 79 (1997) 2237–2240.
[41] F. Robicheaux, M.S. Pindzola, D.C. Griffin, Phys. Rev. Lett. 80 (1998) 1402–1405.
[42] D.C. Griffin, F. Robicheaux, and M.S. Pinzola, Phys. Rev. A 57 (1998) 2798.
[43] C. Bartschat, I. Bray, J. Phys. B: At. Mol. Opt. Phys. 30 (1997) L109–L114.
[44] R.A. Falk, G.H. Dunn, Phys. Rev. A 27 (1983) 754–761.